



Pergamon

Topology Vol. 35, No. 1, pp. 39–54, 1996  
 Copyright © 1995 Elsevier Science Ltd  
 Printed in Great Britain. All rights reserved  
 0040-9383/96 \$15.00 + 0.00

0040-9383(95)00010-0

## ON A CERTAIN TYPE OF COXETER-DYNKIN DIAGRAMS OF PLANE CURVE SINGULARITIES

LUDWIG BALKE and RAINER KAENDERS†

(Received 2 November 1993; in revised form 9 January 1995)

### 0. INTRODUCTION

THE topology of isolated singularities of algebraic plane curves can be studied by means of various invariants. These invariants can be defined more generally for isolated hypersurface singularities. One of these invariants is the set of *Coxeter–Dynkin diagrams* of an isolated hypersurface singularity.‡

The following Fig. 1 gives an impression of how such diagrams look like. Assume that such a singularity is given by a germ of a function, say:

$$f: (\mathbb{C}^{n+1}, 0) \rightarrow (\mathbb{C}, 0).$$

For  $n \geq 3$  the topology of the Milnor fibration belonging to  $f$  is determined by any Coxeter–Dynkin diagram of the singularity. In fact, already the Seifert form of  $f$  (which can be computed from a Coxeter–Dynkin diagram, see e.g. [16]) determines its topological type (see [9]). In contrast, in the case of curve singularities the Seifert form does not determine the topological type, which was recently shown by Françoise Michel and Philippe du Bois [7, 8] (see Fig. 1). They constructed the following example. Let  $f_{rs}$  be the polynomial

$$f_{rs}(x, y) = ((y^2 - x^3)^2 - x^{s+6} - 4yx^{\frac{s+9}{2}}) \cdot ((x^2 - y^5)^2 - y^{r+10} - 4xy^{\frac{r+15}{2}}),$$

where  $r, s$  are odd integers with  $s \geq 11$  and  $s \neq r + 8$ . Then  $f_{rs}$  and  $f_{s-8, r+8}$  have different topological type but isomorphic Seifert forms. The diagrams shown in Fig. 1 belong to these singularities.

On the other hand, for isolated singularities of *irreducible* plane algebraic curves the Coxeter–Dynkin diagrams do determine the topological type of the singularity [6, 19, 16, 20, 21]. It is a very natural question whether the Coxeter–Dynkin diagrams determine the topological type for all singularities. As far as we know this is still an open question for surface singularities. This problem seems to be very difficult.

Whether an analogous statement holds for *reducible* curve singularities and isolated surface singularities is also still an open question, as far as we know.

In dealing with Coxeter–Dynkin diagrams there arise two difficulties. The first is that there is no general method for computing these diagrams and the second is the ambiguity inherent in the definition of these diagrams — the set of all Coxeter–Dynkin diagrams for

†Supported by the EEC within the framework: Human Capital and Mobility.

‡In fact such an invariant can be defined in a still more general situation than in the case of hypersurface singularities, namely for complete intersections (see [10, 11]).

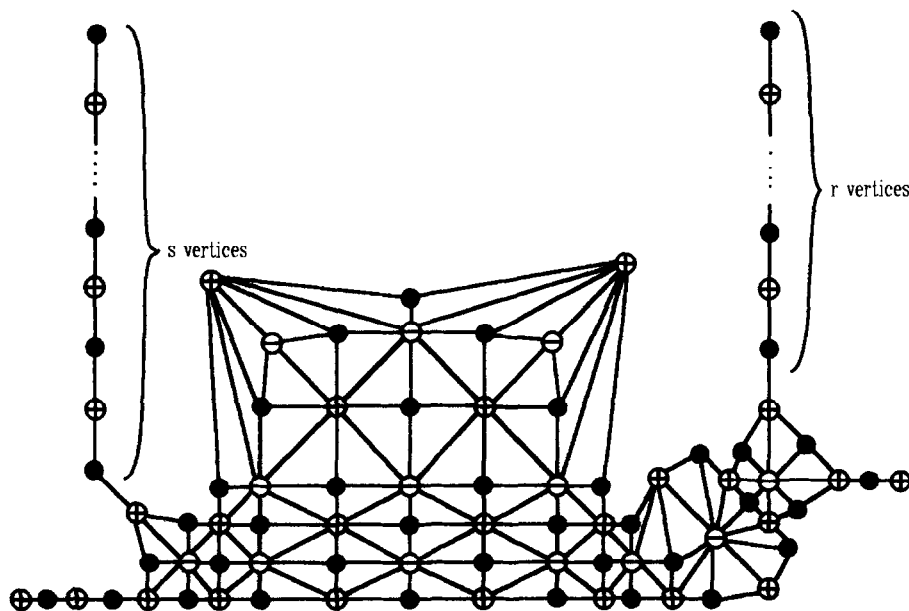


Fig. 1. Example of a Coxeter–Dynkin diagram, which is in particular an  $A\Gamma$ -diagram.

such a singularity is an orbit of a certain braid group acting on the set of Coxeter–Dynkin diagrams with a fixed number of vertices. Except in very few cases this orbit is infinite [4, 16].

But in the case of curve singularities the infinite set of Coxeter–Dynkin diagrams associated with a given singularity contains a certain finite subset of distinguished Coxeter–Dynkin diagrams of a special type. These diagrams were obtained by a beautiful construction of A’Campo [1] and Husein-Zade [15] to compute Coxeter–Dynkin diagrams of a special type. In this article we shall call Coxeter–Dynkin diagrams of this special type *A’Campo–Husein-Zade diagrams* or short  $A\Gamma$ -diagrams (see Definition 1.5). The diagrams shown above are  $A\Gamma$ -diagrams. They were computed by an algorithm of Thomas Schulze-Röbbecke [21].

The geometric construction of these diagrams enables us to see that these diagrams encode information on the topological type of these singularities which we do not see in general Coxeter–Dynkin diagrams. For example it is possible to deduce a precise description of the Seifert form restricted on the radical of the intersection form on the Milnor fibre from these diagrams (see [17]).

The main results of this paper are Theorem 2.5 and Corollary 2.6: *An  $A\Gamma$ -diagram of an isolated plane curve singularity determines the topological type of the singularity.*

This article evolved from work of the second author (see [17]).

## 1. CURVE SINGULARITIES

### 1.1. Coxeter–Dynkin diagrams

According to J. Milnor (see [20]) for any isolated hypersurface singularity

$$f: (\mathbb{C}^{n+1}, 0) \rightarrow (\mathbb{C}, 0)$$

there are positive numbers  $\varepsilon, \eta$ , such that  $f$  induces a locally trivial  $C^\infty$ -fibre bundle

$$\bar{f}: (B_\varepsilon^{2n+2} \cap f^{-1}(B_\eta^2 - \{0\})) \rightarrow B_\eta^2 - \{0\} \quad (1)$$

where  $B_\rho^{2k}$  denotes the open ball of radius  $\rho$  in  $\mathbb{C}^k$  centred at the origin.

If first  $\varepsilon$  and then  $\eta$  are chosen sufficiently small all choices give essentially the same fibre bundle. We call  $\bar{f}$  the *Milnor fibration of  $f$* .

The typical fibre  $F$  of this fibration is called *Milnor fibre*. The middle homology  $H_n(F) = H_n(F, \mathbb{Z})$  is a free abelian group of finite rank. Its rank  $\mu$  is called the *Milnor number*. One has a certain class of distinguished ordered bases. These are obtained from a generic perturbation of  $f$  by means of Picard–Lefschetz theory (cf. [16, 3] (Appendix) or [2]). The elements of such distinguished bases are called “vanishing cycles”.

With respect to such a distinguished basis  $\Delta_1, \dots, \Delta_\mu$  the intersection form  $\mathcal{S}$  on  $H_n(F)$  is described by a graph with weighted edges as follows.

The set of vertices is  $\{1, \dots, \mu\}$ . Two vertices  $i < j$  are joined by an edge with weight  $\mathcal{S}(\Delta_i, \Delta_j)$  if  $\mathcal{S}(\Delta_i, \Delta_j) \neq 0$ . In the graphic representation edges with negative weight are indicated by dotted lines and edges for which no weight is indicated have weight  $\pm 1$ .

The diagrams thus defined are usually called *Dynkin diagrams*. For historical reasons we call them *Coxeter–Dynkin diagrams*.

## 1.2. The method of A’Campo and Husein-Zade

Throughout this article we shall consider singularities of plane curves given by a polynomial  $f \in \mathbb{C}[x, y]$  satisfying the following conditions:

- (i) The hypersurface  $\{(x, y) \in \mathbb{C}^2 \mid f(x, y) = 0\}$  has an isolated singularity in  $0 \in \mathbb{C}^2$ .
- (ii) The decomposition of  $f$  into analytic, irreducible factors is given by polynomials  $f_1, \dots, f_r \in \mathbb{R}[x, y] \subset \mathbb{C}[x, y]$ , i.e.  $f = f_1 \cdots f_r$ . Therefore, the singularity defined by  $f$  only consists of real branches.

A polynomial  $f$  which satisfies these two conditions is called an *admissible* polynomial.

The justification for the restriction to curve singularities of this kind is contained in the following theorem.

**THEOREM 1.1** (see Theorem 3 in [14] or see [1]). *Every isolated plane curve singularity is topologically equivalent (see Theorem 1.3) to a singularity given by an admissible polynomial.*

In order to be able to state the main results of A’Campo and Husein-Zade, we need some technical definitions.

**Definition 1.2** (see [1]). Let  $J$  be the disjoint union of  $r$  copies of the closed unit interval and let  $D_\varepsilon = B_\varepsilon^2 \cap \mathbb{R}^2$ .

A  $C^\infty$ -immersion

$$\alpha: J \rightarrow D_\varepsilon$$

will be called a *partition† of  $D_\varepsilon$  with  $r$  branches*, if it satisfies the following conditions:

- (i)  $\alpha(\partial J) \subset \partial D_\varepsilon$  and  $\alpha(\dot{J}) \subset \dot{D}_\varepsilon$   
 $\alpha(J)$  is connected.

†A’Campo calls it “Partage”.

- (ii) The immersion  $\alpha$  is generic, i.e.  $\alpha(J)$  has only ordinary double points and these lie in the interior of the disc  $D_\epsilon$ .
- (iii) A *region* is a connected component of  $D_\epsilon - \alpha(J)$ . It is required that the following holds for the closure  $\bar{A}$  and  $\bar{B}$  of any two regions  $A$  and  $B$ : either  $\bar{A} \cap \bar{B} = \emptyset$  or  $\bar{A} \cap \bar{B} = \{\text{point}\}$  or  $\bar{A} \cap \bar{B} = \alpha(I)$ , where  $I$  denotes a connected segment of  $J$ .

If the immersion  $\alpha: J \rightarrow D_\epsilon$  is a partition we also call its image in  $D_\epsilon$  a *partition*.

A region is called a *boundary region* (or *exterior region*) if it is adjacent to  $\partial D_\epsilon$ . Otherwise it is called an *interior region*.

We call the images  $\alpha(I)$  where  $I$  is one of the unit intervals of  $J$  a *branch*. By the *intersection number* of two branches  $\alpha(I_1)$  and  $\alpha(I_2)$  we mean the number of elements in  $\alpha(I_1) \cap \alpha(I_2)$ .

A'Campo and Husein-Zade established the following theorem (the decomposition into branches is only given in Husein-Zade's article but it can also be obtained by means of A'Campo's method (see [17])).

**THEOREM 1.3.** (cf. Theorem 4 [14] and Théorème 1 [1]). *Let  $f_0 = f_1 \cdots f_r$  be an admissible polynomial in  $\mathbb{C}[x, y]$  with  $r$  irreducible factors. Then there exist real polynomial deformations*

$$\tilde{f}_v: D_\epsilon \times \mathbb{R} \rightarrow \mathbb{R}, \quad v = 1, \dots, r$$

*of  $f_v$  such that for every  $t \neq 0$  sufficiently small the following holds:*

- (i)  $\tilde{f}_v(x, y; 0) = f_v(x, y)$  for all  $(x, y) \in D_\epsilon$ .

*Let  $\tilde{f}_0 := \tilde{f}_1 \cdots \tilde{f}_r$  be the product and let  $C_t^v$  for  $v = 0, 1, \dots, r$  be the real curve*

$$C_t^v := \{(x, y) \in D_\epsilon \mid \tilde{f}_v(x, y; t) = 0\}.$$

*Then  $C_t^v$  defines a partition. Also,  $C_t^v$  has one branch for  $v = 1, \dots, r$  and  $r$  branches for  $v = 0$ . Also,  $\tilde{f}_{v,t}(x, y) := \tilde{f}_v(x, y, t)$  is a real morsification of  $f_v$ .*

- (ii) *The following relation holds between the Milnor number  $\mu$ , the number  $k$  of double points of  $C_t^0$  and the number  $r$  of branches:*

$$\mu = 2 \cdot k - r + 1.$$

*The function  $\tilde{f}_{0,t}$  has exactly  $\mu$  critical points in  $D_\epsilon$ .*

We are going to define  $\text{AF}$ -diagrams now. We shall do this first for general partitions and then specialise to isolated plane curve singularities. To this end we state:

**PROPOSITION 1.4.** *A partition can be 2-coloured, i.e. it is possible to choose a map from the set of regions into a set of two elements  $\{\ominus, \oplus\}$ , such that the closures of two regions, which are mapped to the same element have never an arc of a branch in common.*

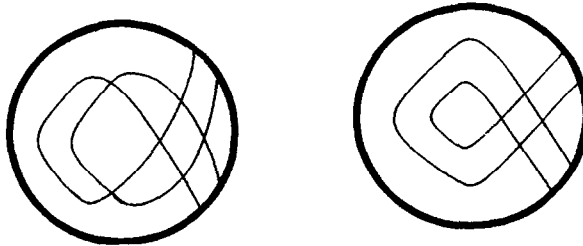


Fig. 2. Examples of the concept of partition: the disc at the left is in contrast to the disc on the right a partition.

For the proof of this proposition, which is straightforward, we refer to [17].  
This allows us to define:

*Definition 1.5.* The *A’Campo–Husein-Zade diagram* of a 2-coloured partition  $\alpha$  ( $A\Gamma$ -*diagram*) is a graph together with a colouring of vertices defined as follows:  
The set of vertices  $V$  of the diagram consists of interior regions and the double-points of the partition  $\alpha$ . The colouring is a map  $\text{sign}: V \rightarrow \{\ominus, \bullet, \oplus\}$ . Restricted to the interior regions it coincides with the 2-colouring of the partition, and for all doublepoints  $v$  we have  $\text{sign}(v) = \bullet$ .

Two such vertices  $P$  and  $Q$  will be connected by an edge, if:

- (i)  $\text{sign}(P) = \ominus$  and  $\text{sign}(Q) = \oplus$   
and the regions  $P$  and  $Q$  have a common boundary segment.
- (ii)  $\text{sign}(P) = \ominus$  and  $\text{sign}(Q) = \bullet$   
and the doublepoint  $Q$  lies at the boundary of the region  $P$ .
- (iii)  $\text{sign}(P) = \bullet$  and  $\text{sign}(Q) = \oplus$   
and the doublepoint  $P$  lies at the boundary of the region  $Q$ .

*Remark:* The diagram we have constructed is an abstract graph with a colouring of its vertices. This graph can be embedded in the disk  $D_e$  in an obvious manner: choose for every interior region a point in the interior of this region. This gives an embedding of the vertices of the  $A\Gamma$ -diagram. (Double points are mapped onto themselves.) We can choose arcs between vertices in the disc which are joined by an edge such that these arcs are Jordon arcs and do not intersect each other except at the endpoints. Moreover, an arc from the chosen point in the interior of a region to some double point should lie in this region.

In this way we have constructed an embedding of the  $A\Gamma$ -diagram into the partitioned disc which is compatible with the partition. The choices we have made are irrelevant with respect to selfhomeomorphisms of the disc which preserve the partition. For a more detailed discussion of embedded  $A\Gamma$ -diagrams see [17, Ch. 1].

*Definition 1.6.* Let  $f_0 = f_1 \cdots f_r$  be a polynomial of  $\mathbb{C}[x, y]$  as in Theorem 1.3. A partition

$$C_t^0 = C_t^1 \cup \cdots \cup C_t^r$$

given by  $\tilde{f}_0 = \tilde{f}_1 \cdots \tilde{f}_r$  as in Theorem 1.3 with properties (i) and (ii) is called a *partition of the singularity*  $f_0$ .

We call the  $A\Gamma$ -diagram associated with such a  $C_t^0$  an *A’Campo–Husein-Zade diagram* ( $A\Gamma$ -diagram) of the singularity  $f_0$ .

From the  $A\Gamma$ -diagram we construct a Dynkin-type diagram as follows. Let  $\mu_\ominus, \mu_\bullet, \mu_\oplus$  be the number of vertices with  $\text{sign} = \ominus, \bullet, \oplus$ , respectively. Replace the vertices  $P$  with  $\text{sign}(P) = \ominus$  by the numbers  $1, \dots, \mu_\ominus$  in any order, replace the vertices  $P$  with  $\text{sign}(P) = \bullet$  by the numbers  $\mu_\ominus + 1, \dots, \mu_\ominus + \mu_\bullet$  in any order and replace the vertices  $P$  with  $\text{sign}(P) = \oplus$  by the numbers  $\mu_\ominus + \mu_\bullet + 1, \dots, \mu_\ominus + \mu_\bullet + \mu_\oplus = \mu$  in any order. More suggestively we can say: replace all vertices by the numbers  $1, \dots, \mu$  according to the rule  $\ominus < \bullet < \oplus$ . Finally, replace all edges by dotted edges.

The main result obtained by A’Campo and Husein-Zade is the following theorem.

**THEOREM 1.7** (cf. Théorème 2, [1] and Theorem 4.1.3, [16]). *The Dynkin-type diagrams*

constructed as above from an  $A\Gamma$ -diagram of the singularity are Coxeter–Dynkin diagrams of the singularity in the sense of Picard–Lefschetz theory.

*Remarks.* A’Campo in [1] uses a different ordering for the elements of a distinguished basis. It is such that  $\oplus < \bullet < \ominus$ . The reason for this is that there are two different conventions for the definition of distinguished bases in the literature. (A’Campo numbers the paths, which are needed to define a distinguished basis anticlockwise (see [1, p. 21, Fig. 5]) while we, like Husein-Zade in [16], do it clockwise. Husein-Zade considers Dynkin diagrams of singularities where the number  $n + 1$  of variables satisfies  $n + 1 \equiv 3 \pmod{4}$ . Such a singularity is obtained from a curve singularity by stabilisation (see [16]). Besides that he chooses in contrast to A’Campo the regular value in the upper half plane of  $\mathbb{C}$ .) (See Fig. 3).

The following proposition relates the structure of the partition obtained in Theorem 1.3 to the decomposition of the singularity into its branches.

**PROPOSITION 1.8.** *Let  $f_0 = f_1 \cdots f_r$  and  $C_i^v$  be as in Theorem 1.3. Then the following statement holds:*

- (i) *The  $C_i^v$ ,  $v = 1, \dots, r$  are also the branches of the partition  $C_i^0$ .*
- (ii) *The intersection number of two branches  $C_i^i$  and  $C_i^j$  of the partition  $C_i^0$  ( $1 \leq i < j \leq r$ ) is the same as the intersection multiplicity of the curve branches  $f_i$  and  $f_j$  with each other.*

*Proof.* (i) This is an immediate consequence of Theorem 1.3 and Definition 1.2.

(ii) The intersection multiplicity  $v(f_i, f_j)$  of  $f_i$  and  $f_j$  is given by the dimension  $\dim_{\mathbb{C}} \mathbb{C}\{x, y\}/(f_i, f_j)$ . We denote by  $\Delta_\eta$  the set  $\{t \in \mathbb{C} \mid |t| < \delta\}$  and name

$$X := \{(x, y, t) \in B_\varepsilon \times \Delta_\eta \mid f_i(x, y, t) = f_j(x, y, t) = 0\}.$$

Then we consider the morphism of complex spaces  $\varphi: X \rightarrow \Delta_\eta$ . It follows from Theorem 1.3 that  $\varphi$  is finite and that  $X$  is a complete intersection. This implies  $(\varphi_* \mathcal{O}_X)_t = \prod_{p \in \varphi^{-1}(t)} \mathcal{O}_{X,p}$  for  $t \in \Delta_\eta$  (cf. [12, 1.10, Lemma 3]). It means moreover that  $\varphi$  is a flat map, which allows us to conclude that the map  $t \mapsto \dim_{\mathbb{C}} (\varphi_* \mathcal{O}_X)_t / \mathfrak{m}_{\Delta_\eta, t} (\varphi_* \mathcal{O}_X)_t$  is a locally constant function on  $\Delta_\eta$  (cf. [12, Corollaries 3.16 and 3.13]). We can complete the proof by noting

$$\frac{(\varphi_* \mathcal{O}_X)_t}{\mathfrak{m}_{\Delta_\eta, t} (\varphi_* \mathcal{O}_X)_t} \otimes_{\mathcal{O}_{\Delta_\eta, t}} \mathbb{C} \cong \prod_{p \in \varphi^{-1}(t)} \mathcal{O}_{\varphi^{-1}(t), p}.$$

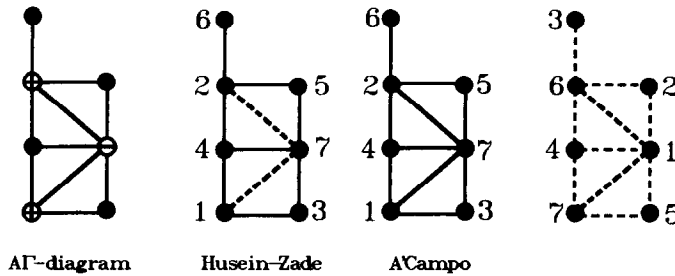


Fig. 3. The example shows an  $A\Gamma$ -diagram for the singularity  $E_7$ . On the right-hand side, we see Coxeter–Dynkin diagrams associated with it by the conventions of Husein-Zade, A’Campo and the one above.

Since in  $p \in \varphi^{-1}(t_0)$  the curves  $\tilde{f}_i(x, y; t_0)$  and  $\tilde{f}_j(x, y; t_0)$  intersect every such point  $p$  is a critical point of  $\tilde{f}_0$  and therefore real. This shows  $\nu(f_i, f_j) = \#(C_i \cap C_j)$ .  $\square$

### 1.3. The topological information

We call two reduced hypersurface singularities

$$f: (\mathbb{C}^n, 0) \rightarrow (\mathbb{C}, 0) \quad \text{and} \quad g: (\mathbb{C}^n, 0) \rightarrow (\mathbb{C}, 0),$$

topologically equivalent (or of the same topological type), if there are representatives  $\bar{f}$  and  $\bar{g}$  of the germs  $f$  and  $g$  on open neighbourhoods  $U$  and  $V$  of  $0 \in \mathbb{C}^n$  as well as a homeomorphism  $\Phi: U \rightarrow V$

$$\Phi: U \rightarrow V$$

with  $\Phi(0) = 0$  such that

$$\Phi(\{z \in U \mid \bar{f}(z) = 0\}) = \{z \in V \mid \bar{g}(z) = 0\}.$$

In the case of curve singularities, e.g. the Puiseux pairs of all the branches together with the intersection multiplicities of the branches with each other are invariants which completely determine the topological type. The topological type of one branch is already determined by its Puiseux pairs (see [5, p. 535 ff. Theorem 21]).

Therefore, we can divide the problem of determining the topological type of such a curve singularity into two parts:

- (i) Determination of the intersection multiplicities of the curve branches with each other.
- (ii) Determination of the topological type of each branch.

Werner Burau has shown in 1932 [6] that the Alexander polynomial of the iterated torus knot of an irreducible curve singularity determines this knot. Therefore, it determines also the topology of the singularity (see [20]). Since this polynomial is also the characteristic polynomial of the monodromy as Milnor showed [20], which can be computed from the Coxeter–Dynkin diagram (see [16]), in the case of an irreducible curve singularity the Dynkin diagram carries the whole topological information. (cf. [19]).

Let us summarize:

**THEOREM 1.9.** *The Coxeter–Dynkin diagrams of the branches of an isolated plane curve singularity together with the intersection multiplicities of the branches with each other determine its topological type.*

Finally, we state (see [13, 14]):

**THEOREM 1.10.** *The Coxeter–Dynkin diagram of an isolated hypersurface singularity is connected.*

## 2. THE $A\Gamma$ -DIAGRAMS DETERMINE THE TOPOLOGICAL TYPE

The discussion in the last section has lead us to the following question: in order to determine the topological type, one has to extract from the  $A\Gamma$ -diagrams the intersection numbers between the respective branches together with their  $A\Gamma$ -diagrams.

Therefore, the following question arises naturally: does the  $A\Gamma$ -diagram—considered as an abstract graph—contain the complete topological information? This section will give a positive answer to this question.

Up to now we have considered an  $A\Gamma$ -diagram  $\Gamma$  as a graph, i.e. as a one-dimensional simplicial complex. But the embedding of this graph into the partitioned disc suggests to transform it into a two-dimensional simplicial complex: fill a 2-simplex into all triangles. These triangles are made up of one double point and two regions. The complex constructed in this way will be denoted by  $\hat{\Gamma}$  and is called an  $A\Gamma$ -complex. In general  $\hat{\Gamma}$  is not homogeneous and can be embedded in the partitioned disc by an embedding extending a choosen embedding of  $\Gamma$ . This subspace of the disc is a deformation retract of the disc, as can be seen by first retracting the boundary regions onto the closure of the union of all interior regions and the branches, and then retracting this set onto the embedded  $A\Gamma$ -complex.

As an embedded graph—not as an abstract graph!— $\Gamma$  determines the partition up to homeomorphism. This can be seen as follows: the partition is determined by the closure of the union of all interior regions and the branches. This topological space is a cell-complex, whose 0-cells are the double points, whose 1-cells are the arcs of branches and whose 2-cells are the interior regions. The 0-cells and the 2-cells and the incidence relation between them are determined by the abstract  $A\Gamma$ -diagram. But the 1-cells and the incidence relation with respect to the other cells are not given by the abstract diagram, but only by an embedding of it into the disc. Since this embedding determines for each region a cyclic ordering of the double points incident with these regions according to an orientation of the disc. For a more detailed discussion of this connection between partitions and  $A\Gamma$ -diagrams, see [17].

We now come to the question how the  $A\Gamma$ -diagram of a partition is related to the diagrams for the branches of that partition, or more generally to the diagram of some subset of these branches. First we fix some notations.

The *star* of a vertex  $v$  is the subcomplex generated by all simplices the vertex is contained in. The *link* of a vertex  $v$  is made up of all simplices of the star which do not contain  $v$ .

What happens if we remove some subset  $A$  of the set  $B$  of branches of the  $A\Gamma$ -diagram  $\Gamma$ ? By this process all double points incident with some branch of  $A$  disappear. Furthermore, two regions separated by an arc of one branch of  $A$  form a new region. If one of these regions was a boundary region the resulting region is also a boundary region. Therefore the set of double points of the partition determined by the branches in  $B \setminus A$  is a subset of the double points of the partition we started with.

*Definition 2.1 (branch structure).* Let  $\alpha$  be a partition with  $A\Gamma$ -diagram  $\Gamma$  and denote by  $B$  the set of branches of  $\alpha$ . The *branch structure* of  $\alpha$  is the family  $(\Gamma_A)_A$  of  $A\Gamma$ -diagrams, where  $A$  runs through all non-empty subsets of  $B$  and  $\Gamma_A$  denotes the  $A\Gamma$ -diagram of the partition  $\alpha_A$  determined by the set of branches  $A$ .

An *equivalence* between two branch structures  $(\Gamma_A)_{A \subseteq B}$  and  $(\Gamma_{A'})_{A' \subseteq B'}$  is a bijection  $\phi: B \rightarrow B'$ , such that  $\Gamma_A$  is isomorphic to  $\Gamma_{\phi(A)}$  as an abstract graph with colouring of vertices for every  $A \subseteq B$ .

**LEMMA 2.2.** *The intersection numbers between the respective branches of a partition together with their  $A\Gamma$ -diagrams are determined by its branch structure.*

*Proof.* We only have to prove that the intersection number of two branches, say  $a$  and  $b$ , can be computed from the branch structure. But according to the remark preceding the



definition of branch structure this number equals the difference between the number of double points of  $\Gamma_{\{a,b\}}$  on the one hand and the sum of the number of double points of  $\Gamma_{\{a\}}$  and  $\Gamma_{\{b\}}$  on the other hand.  $\square$

Simple examples show that in general the branch structure of a partition is not determined by the  $A\Gamma$ -diagram. In Fig. 4 you see an example.

But if we restrict ourselves to partitions and branch structures satisfying some natural additional assumptions, then the branch structure is completely determined by the  $A\Gamma$ -diagram.

*Definition 2.3.* A branch structure  $(\Gamma_A)_A$  is called *connected*, if each graph  $\Gamma_A$  is connected.

A partition is called *reduced* if each branch is incident with at least one double point.

An example of an  $A\Gamma$ -diagram with non-connected branch structure is shown in Fig. 5. As a consequence of Theorems 1.10, 1.3 and 1.7 we obtain the following.

*PROPOSITION 2.4.* A partition belonging to an isolated plane curve singularity as described in Theorem 1.3 is reduced and the corresponding branch structure is connected.

Our main result is the following theorem.

*THEOREM 2.5.* Let  $\alpha, \alpha'$  be reduced partitions having connected branch structures. Their  $A\Gamma$ -diagrams are isomorphic to each other if and only if their respective branch structures are equivalent.

*COROLLARY 2.6.* The topological type of a plane curve singularity is determined by an  $A\Gamma$ -diagram of this singularity.

That the corollary is an immediate consequence of the theorem, is implied by Lemma 2.2 and by Proposition 2.4 which tells us that partitions obtained by the method of A'Campo and Husein-Zade are reduced and have a connected branch structure.

That  $A\Gamma$ -diagrams with equivalent branch structures are isomorphic as abstract graphs, is an immediate consequence of the definition of branch structures and equivalence of branch structures. The rest of this section is devoted to the proof of the converse implication. This will be done by an inductive argument:

We shall split the  $A\Gamma$ -diagram into two suitable parts and apply the induction hypothesis to these parts. In order to elaborate this argument we have to do some preparations.

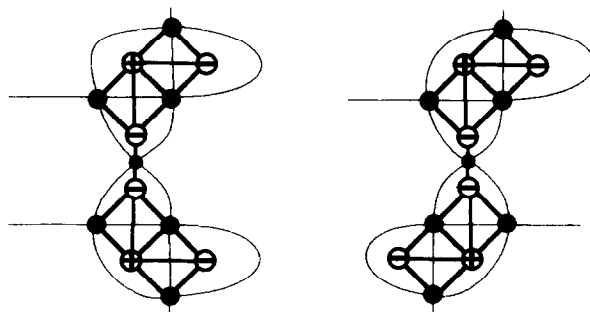


Fig. 4. The branch structure is not determined by the  $A\Gamma$ -diagram.

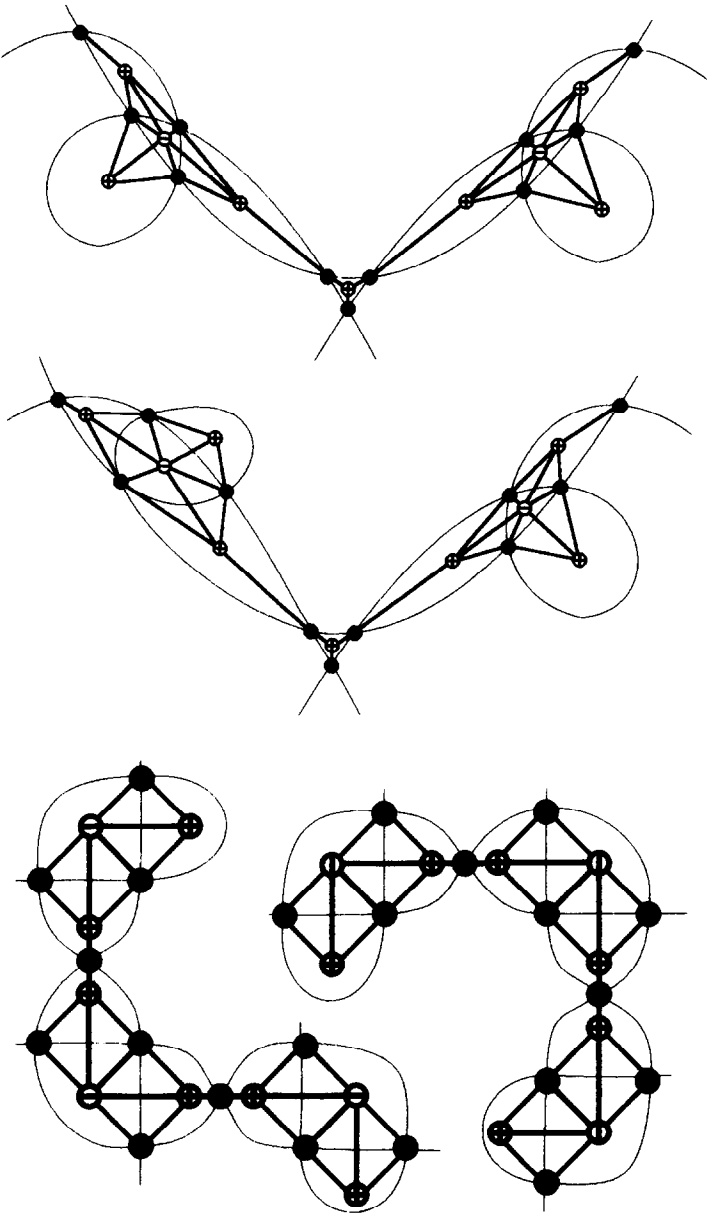


Fig. 5. Examples of  $A\Gamma$ -diagrams with not-connected branch structures.

A *chain* is a connected subgraph  $c$  of the  $A\Gamma$ -diagram  $\Gamma$ , such that each of its vertices is connected by an edge to at most two vertices of the whole diagram and each vertex of  $c$  corresponding to a region is connected to exactly two double points of  $c$ . Moreover, it should contain at least three vertices. Thus, a chain looks like a graph as depicted in Fig. 6.

If we consider  $c$  as subcomplex of  $\hat{\Gamma}$  it has the property that no one of this edges is contained in a 2-simplex. Hence  $c$  can not be a cycle, since otherwise  $\hat{\Gamma}$  would be not simply connected (remember: it is a deformation retract of the disk, as was remarked at the beginning of this section). The double points connected with only one other vertex of  $c$  are called *endpoints* of the chain. Only these endpoints may be connected by an edge to some of the remaining vertices of the diagram.



Fig. 6. A chain.

We say that two vertices  $v_1, v_2$  are *joined by a chain*, if there is a chain in  $\Gamma$ , such that one endpoint is connected by an edge with  $v_1$ , the other one by an edge with  $v_2$ . Since  $\hat{\Gamma}$  is simply connected, removing the chain from  $\Gamma$  yields two connected components  $\Gamma_1, \Gamma_2$  with  $v_i \in \Gamma_i$ . Obviously, the chains of an  $A\Gamma$ -diagram are ordered by inclusion, hence it makes sense to speak of maximal chains.

The operation of *deleting a chain*  $c$  is defined as follows: remove  $c$  and identify those vertices which were connected by an edge to a vertex in  $c$ .

Let  $v$  be a vertex of region type and  $\ell$  one connected component of its link. If the link contains at least two components, the operation of *inserting a chain between  $v$  and  $\ell$*  is defined as follows: replace  $v$  by two copies  $v_1, v_2$ . The vertex  $v_1$  is connected to all vertices of  $\ell$ , the vertex  $v_2$  is connected to the remaining vertices of the link of  $v$ . Then, join  $v_1$  and  $v_2$  by a chain.

These definitions are made only in terms of  $A\Gamma$ -diagrams. But if we let  $\Gamma$  be the  $A\Gamma$ -diagram of a partition  $\alpha$  the notion of chain and the defined operations have a well-defined meaning for partitions themselves—up to homeomorphism: a chain gives rise to a decomposition of the partitioned disc into three discs as shown in Fig. 7. All these three discs are partitioned by restricting  $\alpha$ . The  $A\Gamma$ -diagrams of the leftmost and rightmost partition are obtained by deleting  $v_i$  from  $\Gamma_i$ , respectively, the  $A\Gamma$ -diagram of the middle one is the chain  $c$  we have chosen.

Deleting this chain corresponds to the following operation: remove the interior of the middle disc and glue the remaining two discs along the two arcs  $a, a'$  in the manner which is indicated by the arrows on these arcs.

A region  $v$  is bounded by a sequence of arcs. We have two kinds of arcs: one type of arc separates  $v$  from another interior region and the other one separates  $v$  from a boundary region. If we remove all arcs of the second type, but not their endpoints, then the remaining part of the boundary of  $v$  consists of several components, which may consist of a single double point. These components are cyclically ordered, since they are parts of the boundary of  $v$ , and two consecutive components are joined by an arc of the second type. It is easy to observe that we have a canonical bijection between the vertices of the link of  $v$  in the  $A\Gamma$ -complex  $\hat{\Gamma}$  and the double points and arcs of the first type in the boundary of  $v$ . This bijection maps connected components onto connected components. If we look at the component of the boundary corresponding to  $\ell$ , this component is connected to the rest of the boundary with exactly two arcs of the second type, since there exists other components. These two arcs can be replaced by a chain, and this operation corresponds to inserting a chain between  $v$  and  $\ell$ .

A branch is involved by a chain, if for some region of the chain, one arc bounding this region is part of that branch. The number of branches involved by a chain is one or two. If we want to extract from the branch structure which branches are involved by a chain we must be able to understand each chain in a manner which is compatible with the equivalence of branch structures. The maximal chains of an  $A\Gamma$ -diagram belonging to the branch structure can be identified with some maximal chains of the given  $A\Gamma$ -diagram. The problem is that this identification is in general not unique. But for certain  $A\Gamma$ -diagrams we have uniqueness:

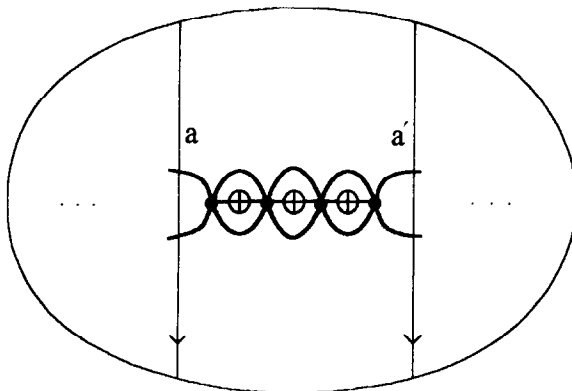


Fig. 7. An embedded chain.

*Definition 2.7.* An  $A\Gamma$ -diagram is called *chain separating* if all maximal chains have pairwise different lengths and inserting of chains does not yield new chains but only lengthens existing ones.

The first condition seems to be non-natural—and indeed many of the  $A\Gamma$ -diagrams of curve singularities are not chain separating. The reasons why we consider such diagrams are as follows. First, for this special class the induction argument which will prove the theorem can be applied. Second, the general case can be reduced to this special case. This is a consequence of the following lemma.

**LEMMA 2.8.** *Each  $A\Gamma$ -diagram can be transformed into a chain separating one by inserting chains. Let  $\alpha, \alpha'$  partitions with chain separating  $A\Gamma$ -diagrams. Furthermore, assume that both branch structures are equivalent and let  $\phi: \Gamma \rightarrow \Gamma'$  denote an isomorphism giving the equivalence. Under these assumptions the following assertion holds: if we delete some chains  $c_1, \dots, c_s$  in  $\alpha$  and their images under  $\phi$  in  $\alpha'$ , then the resulting partitions also have equivalent branch structures.*

*Proof.* The first part is obvious. Since  $\Gamma$  is chain separating we can identify a maximal chain of  $\Gamma_A$  for some subset of branches  $A$  in a canonical manner with a maximal chain of  $\Gamma$ . Hence we know which chains are to be deleted in  $\Gamma_A$  to obtain the corresponding  $A\Gamma$ -diagram for  $\alpha$  after having deleted the chains  $c_1, \dots, c_s$ . This also holds for  $\Gamma'$ . Furthermore, the isomorphisms of  $A\Gamma$ -diagrams induced by the equivalence of branch structures are mapping the chains which are to be deleted onto each other, since all involved  $A\Gamma$ -diagrams are chain separating. Therefore, these isomorphisms yield isomorphisms which are establishing the equivalence of the branch structures after deleting the considered chains.

We now come to the proof of the theorem. We use Lemma 2.8 in order to reduce the general case to the case of chain separating  $A\Gamma$ -diagrams: giving two partitions with  $A\Gamma$ -diagrams which are isomorphic, we insert chains in the first diagram to get a chain separating diagram and make corresponding insertions via an isomorphism in the second  $A\Gamma$ -diagram. The resulting partitions again have isomorphic  $A\Gamma$ -diagrams. If their branch structures are equivalent, then the second part of the above lemma shows that also the given partitions have equivalent branch structures.

The  $A\Gamma$ -complex  $\hat{\Gamma}$  of a chain separating  $A\Gamma$ -diagram  $\Gamma$  is composed of parts of the following four types:

- (i) maximal chains,
- (ii) vertices corresponding to regions, which are connected by only one edge to the endpoint of a chain,
- (iii) discs, i.e. maximal two-dimensional subcomplexes of  $\hat{\Gamma}$ ,
- (iv) vertices corresponding to regions, which are connected to the endpoints of at least three chains.

Since  $\Gamma$  can be identified with the 1-skeleton of  $\hat{\Gamma}$  the  $A\Gamma$ -diagram  $\Gamma$  itself is composed of subgraphs of one of the four types. Parts of  $\Gamma$  which are of one of the latter two types will be called *principal parts*. We prove the theorem by induction on the number of principal parts.

*Beginning of the induction:* Assume that  $\Gamma$  has at most one principal part. If it has none, it is a maximal chain or a maximal chain together with one region connected by an edge to the endpoint of a chain. In both cases the partition  $\alpha$  is determined by  $\Gamma$ . If the only principal part of  $\Gamma$  is a disc, then  $\alpha$  is again determined by  $\Gamma$ , since there is up to homeomorphism only one possibility to embed  $\Gamma$  into a disc.

There remains the case of a region connected to at least three chains. Then all maximal chains will be connected to this region, since in this case  $\Gamma = \hat{\Gamma}$  is a tree. Let  $c_1, \dots, c_s$  be the maximal chains whose other endpoint is connected to a region (which is only connected to that chain) and  $c_{s+1}, \dots, c_{s+r}$  the remaining maximal chains.

Since  $\alpha$  is reduced, we pass twice over double points which are endpoints of chains  $c_{s+i}$  ( $i = 1, \dots, r$ ), if we go along a branch. On the other hand each such endpoint is passed twice by some branch. Hence  $r$  is the number of branches.

The case  $r = 1$  is trivial. Assume now  $r > 1$ .

In the situation we are considering now, the diagram  $\Gamma_A$  is a disjoint union of maximal chains if  $A$  is a proper subset of the set of branches. Since the branch structure is connected, this implies that for such a set of branches either  $\Gamma_A = \emptyset$  or  $\Gamma_A = \{c_i\}$  for some chain  $c_i$ . On the other hand, if  $A = B \cup C$ , then the graph  $\Gamma_B \cup \Gamma_C$  is a subgraph of  $\Gamma_A$ . Furthermore, for each branch  $a_i$ , there exists a branch  $a_j$  such that  $\Gamma_{\{a_i, a_j\}} \neq \emptyset$ , since each branch involved by some chain and each chain involves at most two branches. Hence only in the following cases, the branch structure is connected.

- (i)  $s = 0, r = 3$ : There exist three branches  $a_1, a_2, a_3$  such that  $\Gamma_{\{a_i\}} = \emptyset$  and  $\Gamma_{\{a_i, a_j\}} = c_k$  for  $\{i, j, k\} = \{1, 2, 3\}$ .
- (ii)  $s = 1, r = 2$ : There exist two branches  $a_1, a_2$  such that  $\Gamma_{\{a_1\}} = c_1$  and  $\Gamma_{\{a_2\}} = \emptyset$ .
- (iii)  $s = 2, r = 2$ : There exist two branches  $a_1, a_2$  such that  $\Gamma_{\{a_i\}} = c_i$  for  $i = 1, 2$ .

In all cases the branch structure is determined by the  $A\Gamma$ -diagram itself. Figure 8 shows typical partitions for the situation considered above.

*Induction step:* Assume now that  $\Gamma$  has at least two principal parts. Choose a chain  $c$  connecting two vertices  $v_1, v_2$  contained in principal parts. Hence  $c$  is a maximal chain and the two vertices are contained in different principal parts. The chain  $c$  is given by two arcs which are part of the corresponding branches, say  $a$  and  $b$ . (Note that the case  $a = b$  is not excluded.)

Removing  $c$  yields two components. Their respective union with  $c$  is denoted by  $\tilde{\Gamma}_1$  and  $\tilde{\Gamma}_2$ . The partition  $\alpha$  gives via restriction the partitions  $\tilde{\alpha}_i$  with  $A\Gamma$ -diagram  $\tilde{\Gamma}_i$  ( $i = 1, 2$ ). (In terms of Fig. 7 we restrict  $\alpha$  to the union of the middle disc with the leftmost, respectively, rightmost disc inside the partitioned disc.)

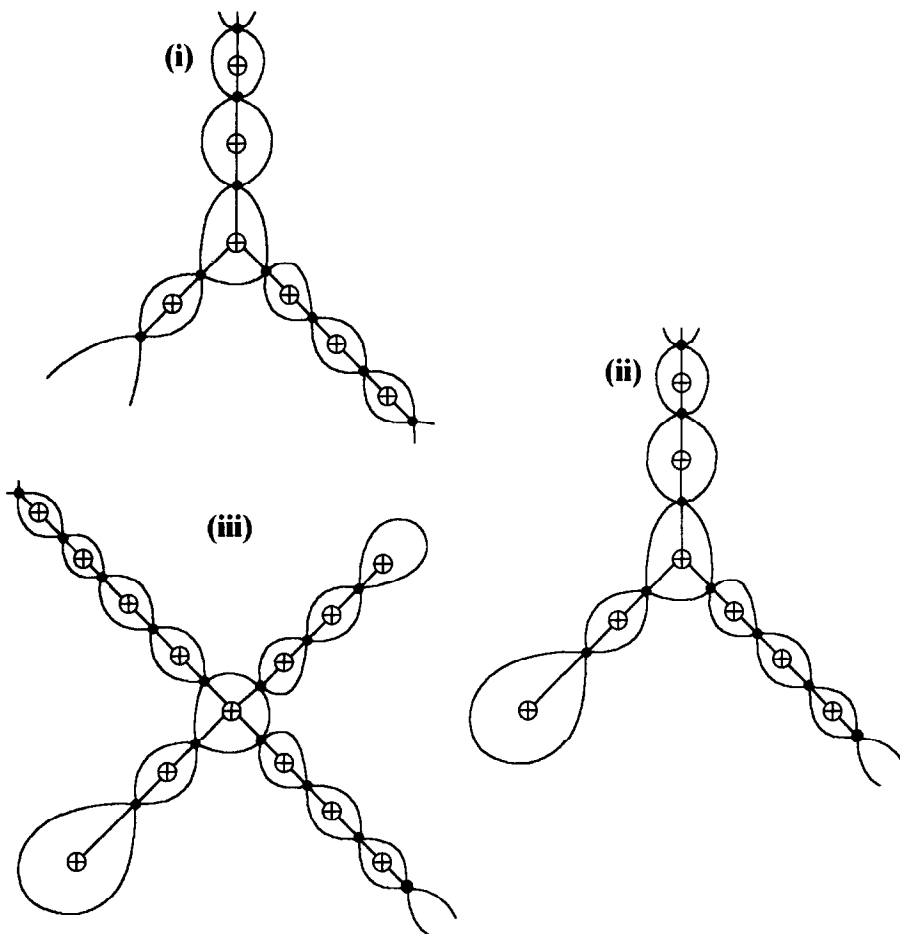


Fig. 8. Typical partitions with one region as principal part.

The chain  $c$  involves in  $\tilde{\alpha}_i$  the branches  $\tilde{a}_i$  and  $\tilde{b}_i$ . If  $a = b$  and  $\tilde{a}_i \neq \tilde{b}_i$  holds, then we define  $\Gamma_i$  by connecting the free endpoint of  $c$  in  $\tilde{\Gamma}_i$  with an additional vertex  $\oplus$  or  $\ominus$ . Otherwise let  $\Gamma_i = \tilde{\Gamma}_i$ . If  $\Gamma_i = \tilde{\Gamma}_i$  let  $\alpha_i = \tilde{\alpha}_i$ ,  $a_i = \tilde{a}_i$ ,  $b_i = \tilde{b}_i$ . Otherwise we obtain  $\alpha_i$  from  $\tilde{\alpha}_i$  by replacing the two arcs of  $\tilde{a}_i$ ,  $\tilde{b}_i$  which are emanating from the double point which corresponds to the free endpoint of  $c$  in  $\tilde{\Gamma}_i$  by a loop starting and ending at this double point. Obviously,  $\Gamma_i$  is the  $A\Gamma$ -diagram of  $\alpha_i$ . The branches  $a_i$ ,  $b_i$  are again the branches of  $\alpha_i$  involved by  $c$ , but in this case we have  $a_i = b_i$ .

We have to do this construction in order to guarantee the equivalence

$$a_i = b_i \Leftrightarrow a = b.$$

Due to the definition of  $\alpha_i$  its set of branches  $B_i$  can be identified with a subset of the set of branches  $B$  of  $\alpha$ . The  $A\Gamma$ -diagram  $\Gamma_A$  for  $A \subseteq B$  can be obtained from the diagrams  $\Gamma_{A \cap B_i}$  of  $\alpha_i$  in the following way.

If  $\{a, b\}$  is not a subset of  $A$ , it is obtained by disjoint union. Otherwise we have to remove the added vertices, if necessary, and to glue the two graphs together along  $c$ .

This description shows, that both  $\alpha_1$  and  $\alpha_2$  must have connected branch structures, since otherwise the branch structure of  $\alpha$  would be non-connected. Due to the choice of  $c$  both  $\Gamma_1$  and  $\Gamma_2$  have a smaller number of principal parts than  $\Gamma$ . Furthermore both  $\alpha_i$  are

reduced and both  $A\Gamma$ -diagrams  $\Gamma_i$  are chain-separating. Hence we can apply the induction hypothesis.

Let  $\alpha'$  be another partition with  $A\Gamma$ -diagram  $\Gamma'$ , which is isomorphic to  $\Gamma$  via the isomorphism  $\psi: \Gamma \rightarrow \Gamma'$ . Let  $c' = \psi(c)$  and apply the above construction to  $\Gamma'$  and  $c'$ . Due to the induction hypothesis we obtain equivalences of branch structures  $\phi_i: B_i \rightarrow B'_i$ . Since  $\Gamma$  and  $\Gamma_i$  are chain separating, we have—after possibly interchanging  $a$  and  $b$ :

$$\phi_1(a_1) = a'_1, \quad \phi_1(b_1) = b'_1, \quad \phi_2(\{a_2, b_2\}) = \{a'_2, b'_2\}. \quad (2)$$

Suppose first  $\phi_2(a_2) = a'_2$ . Then we are able to define a bijection  $\phi: B \rightarrow B'$  by the following rule:

$$\phi(d) = \begin{cases} \phi_1(d), & d \in B_1 \\ \phi_2(d), & d \in B_2. \end{cases}$$

Since  $\phi_i$  is an equivalence of branch structures for  $i = 1, 2$  and due to the construction of  $\Gamma$ , respectively,  $\Gamma'$  from  $\Gamma_i$ , respectively,  $\Gamma'_i$ , this bijection is an equivalence of branch structures.

Assume now that we are not able to choose  $a_1, a_2$  and  $a'_1, a'_2$  in such a way that  $\phi_2(a_2) = a'_2$  together with (2) holds. In that case neither interchanging  $a_1$  and  $b_1$  nor interchanging  $a_2$  and  $b_2$  is an equivalence of the respective branch structures. Hence  $a$  and  $b$  as well as  $a'$  and  $b'$  have to be different branches and we must have  $\phi_2(a_2) = b'_2 \neq a'_2 = \Phi(b_2)$ .

Furthermore, there exists—after possibly interchanging  $a, b$  and  $a', b'$  simultaneously—a subset  $A_1 \subseteq B_1 \setminus \{a_1, b_1\}$  such that  $\Gamma_{A_1 \cup \{a_2\}} \neq \emptyset$  holds in the branch structure of  $\alpha_1$  and a subset  $A_2 \subseteq B_2 \setminus \{a_2, b_2\}$  such that  $\Gamma_{A_2 \cup \{b_2\}} \neq \emptyset$  holds in the branch structure of  $\alpha_2$ . (Note that  $A_i$  may be empty.) Otherwise, there would exist some  $i \in \{1, 2\}$  such that the equality  $\Gamma_A = \emptyset$  would be true for  $A \not\supseteq \{a_i, b_i\}$ . This would imply that interchanging  $a_i$  and  $b_i$  had no effect on the branch structure of  $\alpha_i$ .

Summarising the arguments we can observe for the branch structures of  $\alpha'_1$  respectively  $\alpha'_2$ :

$$\Gamma_{\phi_1(A_1 \cup \{a_1\})} = \Gamma_{\phi_1(A_1) \cup \{a'_1\}} \neq \emptyset, \quad \Gamma_{\phi_2(A_2 \cup \{b_2\})} = \Gamma_{\phi_2(A_2) \cup \{a'_2\}} \neq \emptyset.$$

Because of  $\{a', b'\} \not\subseteq \phi_1(A_1) \cup \phi_2(A_2) \cup \{a'\}$  we obtain that for the branch structure of  $\alpha'$

$$\Gamma_{\phi_1(A_1) \cup \phi_2(A_2) \cup \{a'\}} = \Gamma_{\phi_1(A_1) \cup \{a_1\}} \cup \Gamma_{\phi_2(A_2) \cup \{b_2\}} \quad \text{for } \alpha'$$

is a disjoint union of non-empty graphs and therefore non-connected—in contradiction to our hypothesis on  $\alpha'$ . This completes the proof of the theorem.  $\square$

*Acknowledgements*—The authors are indebted to Egbert Brieskorn and Claus Hertling for stimulating and very helpful discussions.

## REFERENCES

1. N. A'CAMPO: Le groupe de monodromie du déploiement des singularités isolées de courbes planes I, *Math. Ann.* **213** (1975), 1–32.
2. D. BÄTTIG and H. KNÖRRER: *Singularitäten*, Lectures in Mathematics, ETH Zürich, Birkhäuser, Basel, Boston, Stuttgart, (1991).
3. E. BRIESKORN: Die Monodromie der Isolierten Singularitäten von Hyperflächen, *Manuscripta Math.* **2** (1970), 103–161.
4. E. BRIESKORN: Milnor lattices an Dynkin diagrams, *Proc. Sympos. Pure Math.* (Part 1) **40** (1983), 153–165.
5. E. BRIESKORN and H. KNÖRRER: *Plane algebraic curves*, Birkhäuser, Basel, Boston, Stuttgart (1986).
6. W. BURAU: Kennzeichnung der Schlauchknoten, *Abh. Math. Sem. Univ. Hamburg* **9** (1932), 125–133.

7. P. DU BOIS and F. MICHEL: Sur la forme de Seifert des entrelacs algébriques, *C. R. Acad. Sci. Paris Sér. I* **313** (1991), 297–300.
8. P. DU BOIS and F. MICHEL: The integral Seifert form does not determine the topology of plane curve germs, *J. Algebraic Geometry* **3** (1994), 1–38.
9. A. DURFEE: Fibered knots and algebraic singularities, *Topology* **13** (1974), 47–59.
10. W. EBELING: *The monodromy groups of isolated singularities of complete intersections*, Lecture Notes in Math., **1293**, Springer, Berlin (1987).
11. W. EBELING: Vanishing lattices and monodromy groups, *Invent. Math.* **90** (1987), 653–668.
12. G. FISCHER: *Complex analytic geometry*, Lecture Notes in Math. **538** Springer, Berlin (1976).
13. A. M. GABRIÉLOV: Bifurcations, Dynkin diagrams and modality of isolated singularities, *Functional Anal. Appl.* **8** (1974), 94–98.
14. S. M. HUSEIN-ZADE: Dynkin diagrams for singularities of functions of two variables, *Functional Anal. Appl.* **8** (1974), 295–300. *Funktsional Anal. i Prilzhen.* **8** (1974).
15. S. M. HUSEIN-ZADE: Intersection matrices for certain singularities of functions of two variables, *Functional Anal. Appl.* **8** (1974), 10–13. *Funktsional Anal. i Prilzhen.* **8** (1974).
16. S. M. HUSEIN-ZADE: The monodromy groups of isolated singularities of hypersurfaces, *Russian Math. Surveys* **32** (1977), 23–69. *Uspekhi Mat. Nauk.* **32** (1977).
17. R. KAENDERS: Über  $AG$ -Diagramme und Seifertform von Kurven-singularitäten, Master's thesis, Universität Bonn (1992).
18. F. LAZZERI: Some remarks on the Picard-Lefschetz monodromy, in *Quelques journées singulières*, Paris (1974), Centre Math. École Pol.
19. D.T. LÊ: Sur les nœuds algébriques, *Composito Math.* **25** (1972), 281–321.
20. J. MILNOR: *Singular points of complex hypersurfaces*, Ann. of Math. Stud., Vol. **61**. Princeton University Press, Princeton (1968).
21. T. SCHULZE-RÖBBECKE: Algorithmen zur Auflösung und Deformation von Singularitäten ebener Kurven, Master's thesis, Universität Bonn (1977), Bonner Mathematische Schriften, Nr. 96.

*Mathematisches Institut*

*Universität Bonn*

*Wegelerstrasse 10*

*53115 Bonn*

*Germany*

*Mathematisch Instituut*

*Katholieke Universiteit Nijmegen*

*Toernooiveld 1*

*6525 ED Nijmegen*

*The Netherlands*